JOURNAL OF OPTOELECTRONICS AND ADVANCED MATERIALS Vol. 12, No. 10, October 2010, p. 2031 - 2039

A novel design of Butler matrix using optimised size of branch-line coupler

S. K. A. RAHIM, N. M. JIZAT, T. A. RAHMAN, T. K. GEOK[a], A. W. REZA[b*]
Wireless Communication Centre, Fakulti Kejuruteraan Elektrik, Universiti Teknologi Malaysia, 81310 UTM Skudai, Malaysia
[a]*Faculty of Engineering & Technology, Multimedia University, Jalan Ayer Keroh Lama, Bukit Beruang, 75450 Melaka, Malaysia*
[b]*Faculty of Engineering, Department of Electrical Engineering, University of Malaya, 50603 Kuala Lumpur, Malaysia*

Recent development shows that the reduced size couplers are becoming potential building blocks for the growing wireless communications market. This paper presents a new design and realisation of four ports Butler Matrix using the reduced size of branch-line coupler operating at 1.8GHz. The purpose is to reduce the size of branch-line coupler to agree with the application requirements, e.g., mobile applications. Butler Matrix generally consists of branch-line coupler, crossover, and phase shifters. The branch-line coupler has been used as the functional and smart component in constructing the planar of 4×4 Butler Matrix. Using the two-step stubs impedance, the size of the branch-line coupler is optimised in this study. The obtained results show that the area of branch-line coupler has been reduced to 66% compared to the normal size branch-line coupler. Besides, the reduced size coupler shows the same performance like the normal coupler, maintains lower manufacturing cost and miniaturisation in size. The results obtained from this study show satisfactory performance and good agreement with the theoretical results.

(Received September 1, 2010; accepted October 14, 2010)

Keywords: Butler matrix, Branch-line coupler, Beam forming network, Functional and smart material, Smart antenna

1. Introduction

Smart antennas are one of the most promising functional devices in wireless communications [1]. Beam forming networks [2][3] were originated in the late 1950s by Jesse Butler. The beam forming is performed by a device or apparatus, in which energy is radiated by an aperture antenna, is focused at specific direction in space. The Butler Matrix is a microwave network, employed in beam forming and scanning network. It consists of hybrid couplers, cross couplers, and phase shifters [4]. This feed network takes the form of four inputs and four outputs connection. A signal inputted at different input ports in a Butler Matrix produces different phase tapers among the output ports.

The size reduction of branch-line coupler technique using eight two-step stubs has been reported in [5]. In comparison to conventional hybrid couplers, the reduced size coupler offers lower insertion loss and higher compactness (a significant reduction of 25% in the circuit area) [5]. Additional degrees of design choice can be obtained by including shunt open stubs and all these are the reasons for the major reduction in size. The reduced size couplers are potential elements for the growing wireless communications market [6].

Butler Matrix is a beam forming network that comprises of quadrature coupler, crossover, and phase shifters [7]. By using narrow beams, it is possible to increase the gain in the desired signal direction and to reduce it toward the interference directions [8]. Different structures of multiple–beam networks (beamformers) have been reported in the literature, such as the Blass matrix [9], the Nolen matrix [10], the Rotman lens [11], and the Butler Matrix system [12].

In this paper, a new design for reducing the size of branch-line coupler using eight two-step stubs is proposed. Therefore, each input port of the Butler Matrix is divided into four output ports with equal amplitude and the specified relative phase differences, consequently generating four different beams through the connected smart antenna array. The potential advantages of the proposed method are as follows. First, it can be implemented easily using the hybrid and the phase shifter. Second, the generated beams are orthogonal of the Woodward-Lawson type and have narrow beamwidth and high directivity. Third, it has minimum path length and number of components compared to other uniform excitation beamforming networks. Fourth, it has a high and almost constant beam crossover level, which does not change with the frequency. This guarantees a good coverage pattern and full system gain at any point in the coverage area [13].

The organisation of the remaining part of this paper is as follows: Section 2 describes the theories and the proposed methodology to optimise the size of the branch-line coupler that includes the detailed mathematical calculation and simulation process. Section 3 discusses the results obtained from this simulation study and the detailed analysis. Lastly, Section 4 provides the concluding remarks and future guideline.

2. Methodology

A branch-line coupler with two-section stubs consisting of high and low impedance transmission lines for the ease of interconnection of low impedance transmission lines is presented in [1][14]. According to the transmission theory, almost the same frequency characteristics as those of a normal branch-line coupler can be obtained, although there are slight differences in the high-frequency region over the centre frequency. The line length was reduced to 50% and the experimental circuit was reduced to 25% in area, and frequency characteristics show good agreement with the theoretical results.

For the mathematical calculation (may refer to our paper [15][16] and also I. Sakagami [1][14]), this paper proposes a new electrical length, due to optimisation purpose. Besides that, in this study, the reduced size branch-line coupler has been integrated finally with crossover and phase shifters to implement the reduced size Butler Matrix (explained later in Section 3). In this paper, Zo, Z_a, Z_b, and Z_c denote the characteristic impedances, and $90^{\circ}, \theta_a$, and θ_b denote the electrical lengths at the centre frequency.

2.1 Single stub

Using the F-matrices, the equivalent conditions ($F^{f2} = F^{f3}$) at the centre can be derived using the following equations [1]:

$$F^{f2} = \frac{1}{\sqrt{2}} \begin{bmatrix} 1 & jZo \\ jYo & 1 \end{bmatrix} \quad (1)$$

$$F^{f3} = \begin{bmatrix} 1 & 0 \\ jYb\tan\theta b & 1 \end{bmatrix} \begin{bmatrix} \cos\theta a & jZa\sin\theta a \\ jYa\sin\theta a & \cos\theta a \end{bmatrix} \times \begin{bmatrix} 1 & 0 \\ jYb\tan\theta b & 1 \end{bmatrix} \quad (2)$$

From equations (1) and (2), we obtain [1][14][15]:

$$Z_a = \frac{Zo}{\sqrt{2}\ \sin\theta a} \quad (3)$$

$$Z_b = \frac{Zo\ \tan\theta b}{\sqrt{2}\ \cos\theta a - 1} \quad (4)$$

$$Z_c = \frac{Z_b}{2} \quad (5)$$

When the branch-line coupler behaves as a 3dB coupler in a 50Ω system, the characteristic impedances must be:

$$Zo = Z_{br} = 50\Omega \text{ and } Z_{th} = \frac{50}{2^{0.5}} = 35.36\Omega$$

where Z_{br} is the characteristic impedance for branch-line and Z_{th} is the characteristic impedance for through-line.

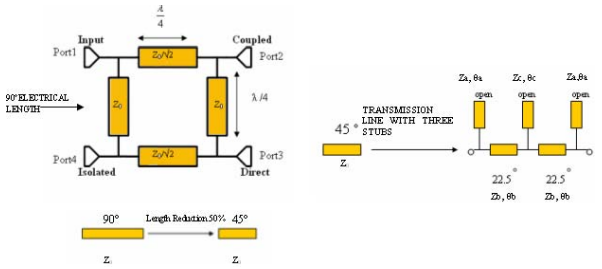

Fig. 1. Line reduction.

From Fig. 1, if the reduction of the line-length is set at 50%, therefore, the obtained θa is 22.5˚.

For the case of a stub at a corner of the branch-line coupler, the following equation (6) is used. Since the characteristic impedance Zb^{cor} of the stubs at four corners is given by the parallel connection of branch-line and through-line, namely, Zb^{br} and Zb^{th} as below [14][15]:

$$Zb^{cor} = Zb^{br}Zb^{th} / (Zb^{br} + Zb^{th}) \quad (6)$$

2.2 Two-step stubs

By applying the circuit in Fig. 1 to the normal branch-line coupler, we can obtain the reduced size branch-line coupler with eight single stubs. However, the impedance of a stub tends to become low of 20 or 30 Ω [14][15]. Therefore, to make the connection easier, the stub is transformed into the circuit, consisting of a two-step structure of high and low impedance sections.

Before carrying out fundamental analysis, it is appropriate to define several symbols. In this study, the parameters, such as Y_{sg}, Y_{stl}, and Y_{st2} are the characteristic admittances, and θ_{sg}, θ_{st1}, and θ_{st2} denote the electrical lengths at the centre. The Y_{sg}^{in} and Y_{st}^{in} are the input admittances.

By applying following equation (7), an open end stub can be designed and transformed into two-step 'n' stubs system [14][15].

$$Y_{sg}\tan\theta_{sg} = \frac{Y_{st1}\tan\theta_{st1} + nY_{st2}\tan\theta_{st2}}{1 - nY_{st2}Z_{st1}\tan\theta_{st1}\tan\theta_{st2}} \quad (7)$$

where n indicates the number of transmission lines in the second section.

2.3 Calculation of impedance and electrical length

2.3.1 Single stub

Applying Zo = 50 Ω to equations (3), (4) and (5), we obtain:

$$Za^{br} = \frac{50}{\sqrt{2}\ \sin 22.5^{\circ}} = 92.4\ \Omega$$

$$Zb^{br}=\frac{50 \quad \tan 20°}{\sqrt{2} \quad \cos 22.5°-1}=59.4\ \Omega$$

$$Zc^{br}=\frac{59.4\Omega}{2}=29.7\ \Omega$$

Next, by substituting Z_{th} = 35.36 Ω to equations (3), (4) and (5), we obtain:

$$Za^{th}=\frac{35.36}{\sqrt{2} \quad \sin 22.5°}=65.3\ \Omega$$

$$Zb^{th}=\frac{35.36 \quad \tan 20°}{\sqrt{2} \quad \cos 22.5°-1}=42\ \Omega$$

$$Zc^{th}=\frac{42\Omega}{2}=21\ \Omega$$

Therefore, by applying equation (6), the obtained characteristic impedance for the corner stubs is,

$$Zb^{cor}=24.6\ \Omega$$

2.3.2 Two-step stubs

The stub impedances calculated above are Zc^{br}=29.7Ω, Zc^{th}=21Ω, and Zb^{cor} = 24.6Ω. A low-impedance stub is transformed into a two-step structure, according to equation (7). The line parameters are indicated in Table 1 [5] and Fig. 2 explains the symbols used for the line parameters [1][5].

(a) For branch-line (Zc^{br}) impedance transformation,

let Z_{st1}=80Ω, θ_{st1} =10°, θ_{st2} =8°, and n=3.

Therefore,

$$Y_{st1}=\frac{1}{Z_{st1}}=\frac{1}{80\Omega}=0.0125\text{S}$$

$$Y_{sg}=\frac{1}{Zc^{br}}=\frac{1}{29.7\Omega}=0.0337\text{S; and } \theta_{sg}=20^{\circ}$$

By substituting the above values in equation (7), we obtain:

$$0.0337 \tan 20^{o}=\frac{0.0125 \tan\ 10^{o}+3\ Y_{st2} \tan\ 8^{o}}{1\text{-}3\ Y_{st2}(80) \tan\ 10^{o} \tan\ 8^{o}}$$

Therefore, Y_{st2} = 0.0203S and

$$Z_{st2}=Z_2^{br}=\frac{1}{0.0203}=49.17\ \Omega$$

(b) For through-line (Zc^{th}) impedance transformation,

let Z_{st1}=80Ω, θ_{st1} =10°, θ_{st2} =11°, and n=3.

Therefore, $Y_{st1}=\frac{1}{Z_{st1}}=\frac{1}{80\Omega}=0.0125\text{S}$

$$Y_{sg}=\frac{1}{Zc^{th}}=\frac{1}{21\Omega}=0.0476\text{S; and } \theta_{sg}=20^{\circ}$$

By substituting the values in equation (7), we get the following:

$$0.0476 \tan 20^{o}=\frac{0.0125 \tan\ 10^{o}+3\ Y_{st2} \tan\ 11^{o}}{1\text{-}3\ Y_{st2}(80) \tan\ 10^{o} \tan\ 11^{o}}$$

Therefore, Y_{st2} = 0.02083S and

$$Z_{st2}=Z_2^{th}=\frac{1}{0.02083}=47.95\ \Omega$$

(c) For corner stub (Zb^{cor}) impedance transformation,

let θ_{st1}=7.07°, θ_{st2} = 15°, and n=2.

Therefore, $Y_{st1}=\frac{1}{Z_{st1}}=\frac{1}{60\Omega}=0.0167\text{S}$

$$Y_{sg}=\frac{1}{Zb^{cor}}=\frac{1}{24.6\Omega}=0.0407\text{S; and } \theta_{sg}=20^{\circ}$$

By substituting the values in equation (7),

$$0.0407 \tan 20^{o}=\frac{0.0167 \tan 7.07^{o}+2\ Y_{st2} \tan 15^{o}}{1\text{-}2\ Y_{st2}(60) \tan 7.07^{o} \tan 15^{o}}$$

Therefore, Y_{st2} = 0.0214S and

$$Z_{st2}=Z_2^{cor}=\frac{1}{0.0214}=46.72\ \Omega.$$

Table1. The line parameters used for symbols in Fig. 2 [5].

Za^{br}	θa	Z_1^{br}	θ_1^{br}	Z_2^{br}	θ_2^{br}
92.39	22.5°	80	10°	49.17	8°
Za^{th}	θa	Z_1^{th}	θ_1^{th}	Z_2^{th}	θ_2^{th}
65.33	22.5°	80	10°	47.95	11°
Z_1^{cor}	θ_{c1}	Z_2^{cor}	θ_{c2}		
60	7.07°	46.72	15°		

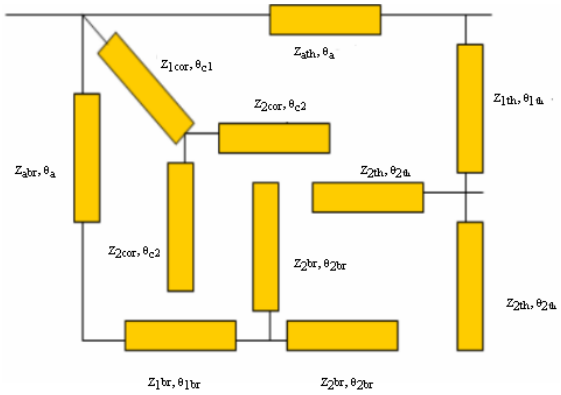

Fig. 2. The symbols for the line parameters [5].

2.4 Calculation of width and length

Each width and length of transmission line of the branch-line coupler is computed by using the TX Line tool from the Applied Research Wave (AWR) by key in the characteristics of the flame resistance board (FR4 Board), which is the effective dielectric constant ξ_r = 4.6, dielectric thickness=1.6mm, metal thickness T= 0.035mm, dielectric of copper=5.88E+07, loss tangent=0.019, frequency operated=1.8GHz, and impedance and electrical length of every part of transmission line of branch-line coupler that have been calculated. Table 2 shows the calculated values of the width and the length for the reduced size branch-line coupler.

Table 2. The calculated values of width and length.

TX Line	Impedance(Ω)	Electrical Length	Width (mm)		Length (mm)	
			Before tuning	After tuning	Before Tuning	After Tuning
Za^{br}	92.39	22.5 °	0.7863	0.7863	5.879	5.879
Za^{th}	65.33	22.5 °	1.778	1.778	5.715	5.715
Z_1^{cor}	60	7.07 °	2.102	1.034	1.783	2.5
Z_1^{br}	80	10 °	1.139	0.576	2.583	2.872
Z_1^{th}	80	10 °	1.139	1.1	2.583	2.583
Z_2^{cor}	46.72	15 °	3.269	1	3.706	2.3
Z_2^{br}	49.17	8 °	3.002	3.002	1.985	1.7865
Z_2^{th}	47.95	11 °	3.132	2.1	2.723	2.1

3. Results and discussion

The simulation has been performed using the Advanced Design System (ADS) software, which evaluates the characteristics of the Butler Matrix. The performance of the normal branch-line coupler, reduced size branch-line coupler, crossover, phase shifter and Butler Matrix operating at 1.8GHz will be presented in this section. The substrate that is used to fabricate these couplers is the FR4 Board (ξ_r =4.6, thickness =1.6 mm, and T = 0.035), where these values are used while designing the schematic diagram and layout.

3.1 Performance analysis of branch-line coupler

3.1.1 Normal branch-line coupler

Quadrature coupler has important characteristics, and it is widely used in microwave circuits, such as power combiners and dividers, balanced mixers, balanced amplifiers, feed networks in antenna arrays, image-rejection mixers, and balanced amplifiers [17]. In this study, a normal branch-line coupler is presented using the schematic design. Figs. 3(a) and 3(b) show the schematic diagram and layout of the normal size branch-line coupler, respectively, which operates at 1.8GHz. Fig. 4 shows the S-parameter and phase difference between the output ports. It is observed that, the phase difference between the output Port 3 and Port 2 is 90˚.

3.1.2 Reduced size branch-line coupler

A reduced size branch-line coupler using two-step stubs impedance is presented using the schematic diagram and layout, respectively as shown in Figs. 5(a) and 5(b). Fig. 6 shows the S-parameter and phase difference between the output ports of the reduced size branch-line coupler. It shows the phase difference between the output Port 3 and Port 2 is 90˚.

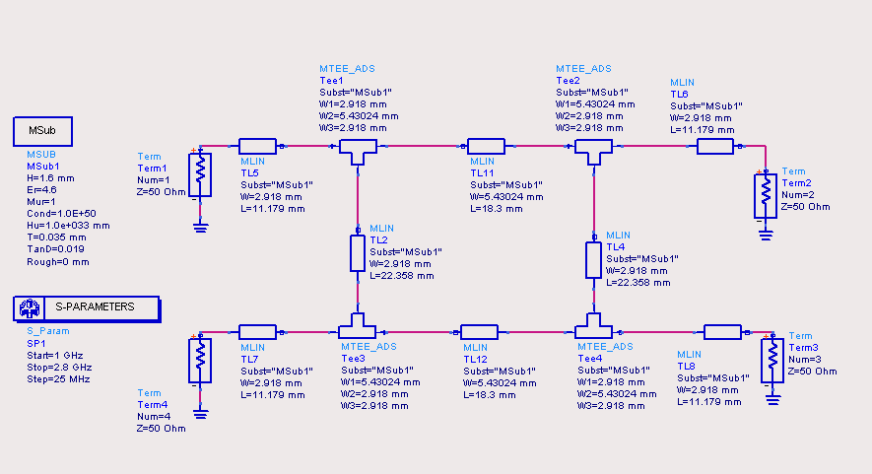

(a)

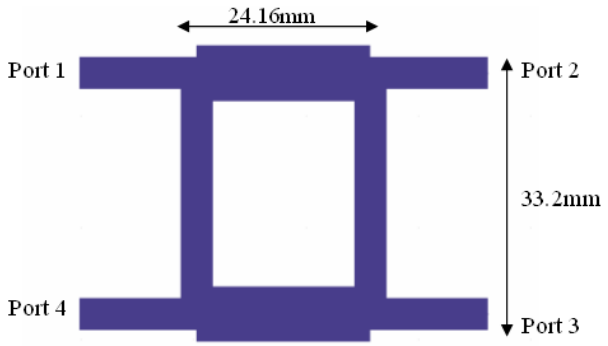

(b)

Fig. 3. Normal branch-line coupler (a) Schematic diagram; (b) Layout.

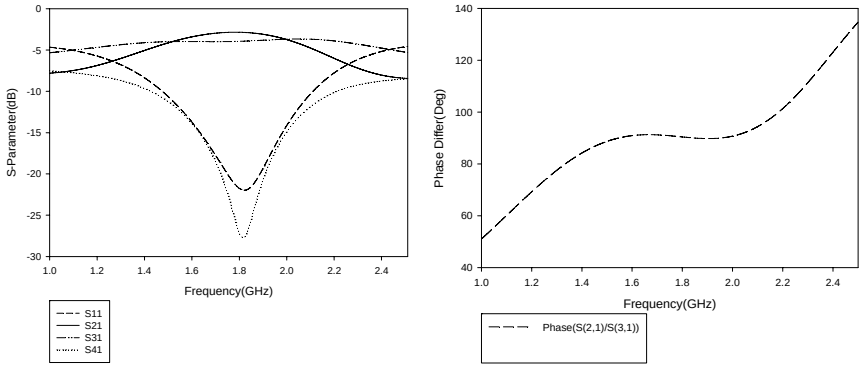

Fig. 4. S-Parameter and phase difference between output ports of normal branch-line coupler.

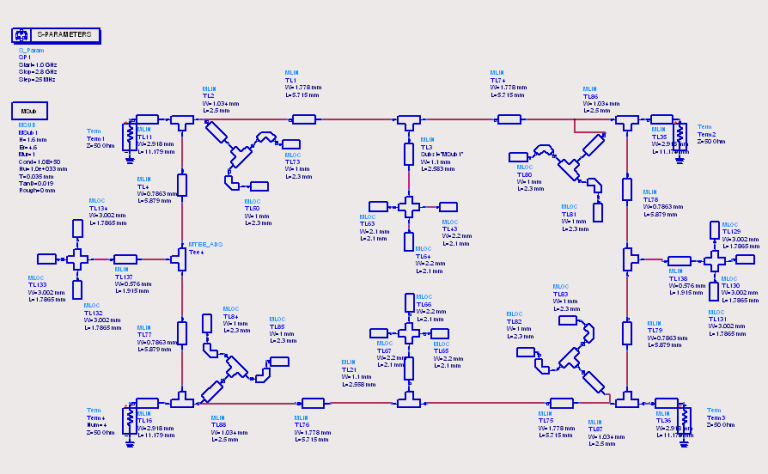

(a)

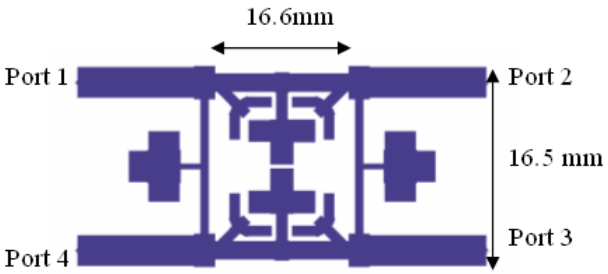

(b)

Fig. 5. The reduced size branch-line coupler (a) Schematic diagram; (b) Layout.

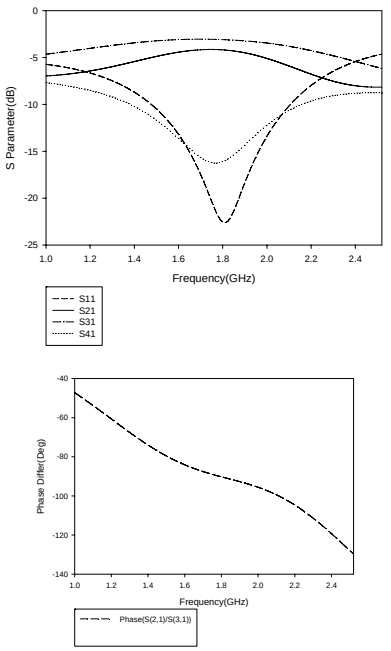

Fig. 6. S-Parameter and phase difference between output ports of the reduced size branch-line coupler.

In summary,

i) The normal branch-line coupler provides 24.61mm × 33.2 mm =817 mm^2 in area while the reduced size of branch-line coupler shows the design of 16.6mm×16.5mm=273.9 mm^2. The proposed design shows that the area of branch-line has been reduced by:

$$\frac{(817-273.9)}{817}\times 100\ \%=66.47\%$$

ii) The normal branch-line coupler and the reduced size of branch-line coupler give the same performance in terms of reflection coefficient and S-parameter analysis as follows. The simulated S-parameters in Figs. 4 and 6 show the return loss (S_{11}) of -21dB for the normal and the reduced size branch-line coupler.

$$RL = 20\log[r]$$
$$-21=20\log[r]$$
$$r=0.08$$

$$\text{Transmitted power} = [1-[r]^2]\times 100\% = 99.34\%$$

Here, *RL* is the return loss and *r* is the reflection coefficient.

iii) The phase difference between the Port 2 and the Port 3 is 90˚.

iv) The expression S_{21} in connection with couplers means an equal distribution of power between the two (output) ports of the coupler with respect to an input port. Hence, a 3 dB coupler is a "hybrid", as shown below:

$$10\log (Power_{out}/Power_{in}) = -3 \text{ dB}$$

$$Power_{out}/Power_{in} = 10^{(-3/10)} = 0.5$$

Therefore, the output power $Power_{out}$ of one of the output ports is half (-3 dB) of the input power $Power_{in}$; the other half emerges from other output port. The Port 1 is the input port, then Port 3 is said to be the coupled port, and Port 2 is said to be the direct port with half of the input power being output from each of the output ports. The Port 4 is said to be isolated from Port 1.

3.2 Crossover

The 0 dB crossover is made up of two 3 dB branch-line cascaded couplers, which produce the minimal coupling between them. Figs. 7(a) and 7(b) show the schematic diagram and layout, respectively of the crossover by cascading two branch-line couplers. Fig. 8 shows the S-parameter and phase difference between the output ports of crossover is 90˚.

The signal entering input Port1 is divided into two equal parts by the first branch-line coupler and recombined by the second branch-line coupler towards Port 3 with 90˚ phase shift. The simulated results show that S_{31} gives the value of 0 dB, minimal coupling between two branch-line coupler. The reflection coefficient and S_{11} show that the transmitted power at Port 1 is satisfactory.

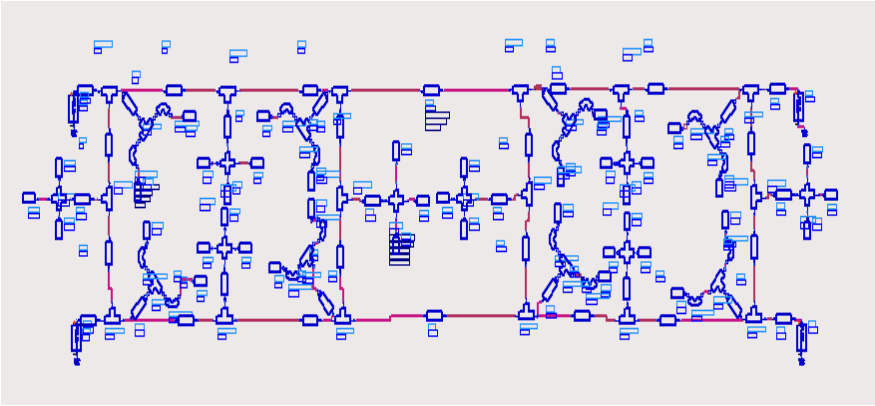

(a)

(b)

Fig. 7. Crossover (a) Schematic diagram; (b) Layout.

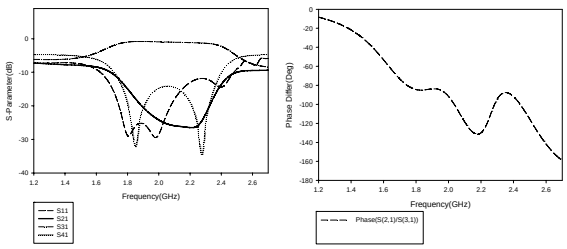

Fig. 8. S-Parameter and phase difference between output ports of crossover.

Fig. 9. Layout of 45° phase shifter.

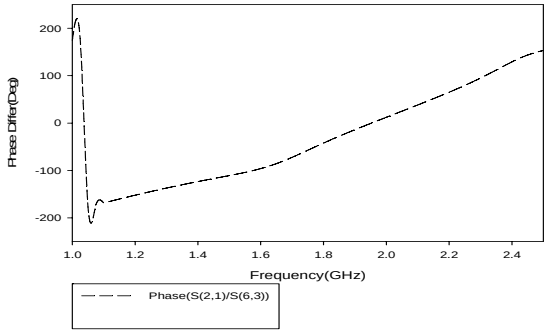

Fig. 10. Phase difference between output ports of 45° phase shifter.

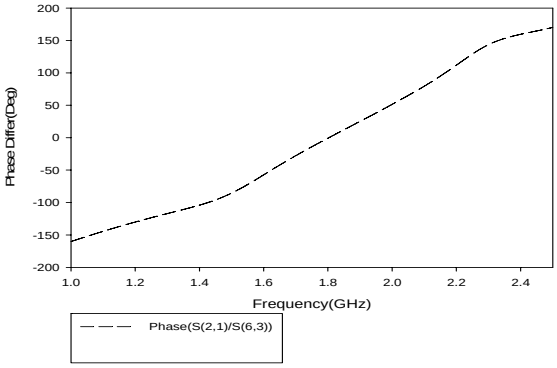

Fig. 11. Phase difference between output ports of 0˚ phase shifter.

3.3 Phase shifter

3.3.1 Forty five degree phase shifter

A phase shifter makes a change in the phase angle of wave transmission. The 45˚ phase shifter is designed by using the transmission line with crossover until the phase difference between the Port (6, 3) and Port (2, 1) is 45˚. Figure 9 presents the layout of 45˚ phase shifter while Fig. 10 shows the phase difference of 45˚.

3.3.2 Zero degree phase shifter

The 0˚ phase shifter is designed as the same way as designing the 45˚ phase shifter but changing the transmission line until the phase difference between the transmission lines with crossover is 0˚. Figure 11 shows the phase difference between Port (6, 3) and Port (2, 1) is 0˚.

3.4 Design of a Butler matrix

Finally, a 4×4 Butler matrix has been successfully designed. The crossover and 0˚ and 45˚ phase shifters are integrated with the branch-line coupler to implement the architecture of a 4×4 Butler Matrix. Fig. 12 presents the layout of the proposed Butler Matrix. Fig. 13 illustrates the fabricated Butler Matrix and square patch array antenna. In this study, the square patch antenna operating at 1.8 GHz is designed using the ADS as stated earlier. The design consideration of the patch antenna on microstrip includes a substrate of 4.6 and the thickness of 1.6 mm with a loss tangent of 0.019.

Fig. 14 shows the S-parameter of Butler Matrix while Fig. 15 shows the phase differences between different ports (i.e., Port 1 to Port 4) with the theoretical and the simulated results. The measurement results of the Butler Matrix for S-parameter are presented in Fig. 16. It is observed from the figure that, the obtained S_{11} is below -10dB, which indicates good performance of the transmitted signal.

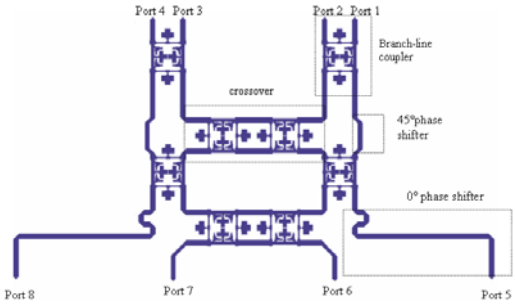

Fig. 12. Layout of Butler matrix.

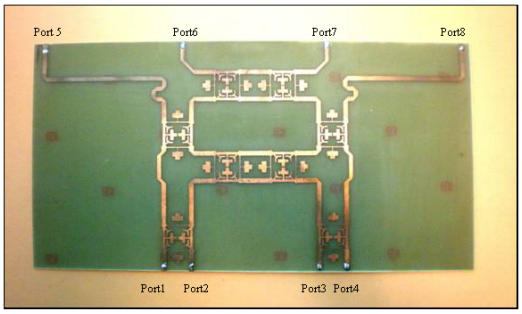

Fig. 13. Fabricated Butler matrix and square patch array antenna.

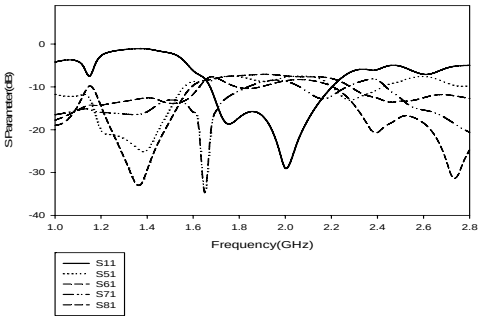

Fig. 14. S-parameter analysis of Butler matrix.

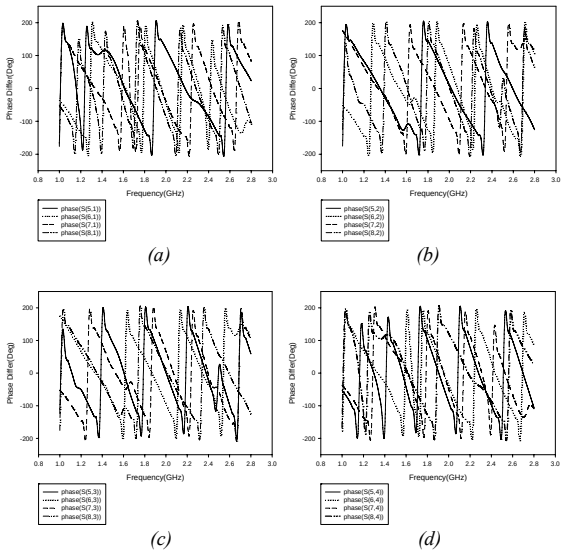

Fig. 15(a-d). Phase differences between different ports with theoretical and simulated values.

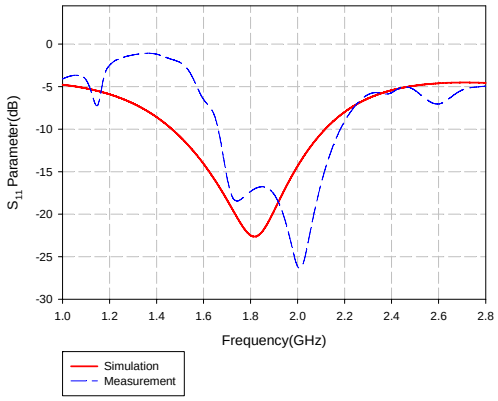

Fig. 16. S_{11} measurement results of Butler matrix.

4. Conclusions

A new design for 4×4 Butler Matrix using reduced size of branch-line coupler has been presented in this paper. The obtained results show that, the proposed design has reduced the area of branch-line coupler to 66% (which is much better than the results obtained by our work as reported in [15] and also by I. Sakagami [1][5][14]) without having to compromise the circuit performances as compared to the normal branch-line coupler. The proposed design yields the same performance in terms of reflection coefficient and S-parameter analysis in comparison with the normal branch-line coupler. Thus, the technique presented in this paper will be very useful to implement the design of Butler Matrix, which is optimum in size. For the future work, the design of Butler Matrix can be realised onto other material, such as Duroid, Rodgers or Ceramic. Moreover, further investigation on low noise amplifier (LNA) can be completed to perform the best radiation pattern for each output port.

Acknowledgements

This research work is financially supported by Ministry of Science, Technology and Innovation (MOSTI), Malaysia through the fostering project of Smart Antenna System.

References

[1] I. Sakagami, M. Haga, T. Munehiro, IEE Proc-Microw. Antennas Propag. **146**, 455 (1999).
[2] S. Shamsinejad, M. Soleimani, N. Komjani, Progress In Electromagnetics Research Letters **3**, 43 (2008).
[3] C. W. Tang, M. G. Chen, IEEE Transactions on Microwave Theory and Techniques **55**, 9 (2007).
[4] P. Q. Mariadoss, M. K. A. Rahim, M. Z. A. A. Aziz, IEEE Asia Pacific Microwave Conference **5**, 4 (2005).
[5] S. Z. Zhang, A. Tokunou, I. Sakagami, IEEE Asia Pacific Microwave Conference, Sydney, Australia, 1281 (2000).
[6] N. Wall, ITS Comms - The CALM and Efficient Way, Traffic Engineering & Control Magazine (2006). J. Clerk Maxwell, A Treatise on Electricity and Magnetism, 3rd ed. **2,** 68 (1892), Oxford, Clarendon.
[7] T. N. Kaifas, J. N. Sahalos, IEEE Antennas and Propagation Magazine **48,** 93 (2006).
[8] M. Nedil, T. A. Denidni, L. Talbi, IEEE Transaction on Microwave Theory and Techniques **54**, 499 (2006).
[9] S. Mosca, F. Bilotti, A. Toscano, L. Vegni, IEEE Trans. Antennas Propag. **50**, 225 (2002).
[10] Y. T. Lo, S. W. Lee, Antenna Handbook, Van Nostrand Reinhold, New York 1988.
[11] W. Rotman, R. F. Turner, IEEE Trans. Antennas Propag. **11**, 623 (1963).
[12] T. A. Denidni, T. E. Libar, IEEE Proc. Personal, Indoor and Mobile Radio Communications, 2461 (2003).
[13] A. M. El-Tager, M. A. Eleiwa, Progress In Electromagnetics Research Symposium, Beijing, China, 571 (2009).
[14] I. Sakagami, R. Teraoka, T. Munehiro, IEEE Microwave Conference Asia Pacific **5P16-4**, Hong Kong, 1137 (1997).
[15] N. A. Muhammad, S. K. A. Rahim, N. M. Jizat, T. A. Rahman, K. G. Tan, A. W. Reza, Wireless Personal Communications, DOI: 10.1007/s11277-010-0164- 817 (2010) (in press).
[16] Rahim, S. K. A., Muhammad, N. A., Rahman, T. A., Proceedings of the Fourth European Conference on Antennas and Propagation (EuCAP), Barcelona, Spain, 1 (2010).
[17] M. Bona, L. Manholm, J. P. Starski, IEEE Trans. Microwave Theory and Tech. **50**, 2069 (2002).

*Corresponding author: awreza98@yahoo.com